



HAL
open science

Stark Broadening from Impact Theory to Simulations

Roland Stamm, Ibtissem Hannachi, Mutia Meireni, Laurence
Godbert-Mouret, Mohammed Koubiti, Yannick Marandet, Joël Rosato, Milan
Dimitrijević, Zoran Simić

► **To cite this version:**

Roland Stamm, Ibtissem Hannachi, Mutia Meireni, Laurence Godbert-Mouret, Mohammed Koubiti, et al.. Stark Broadening from Impact Theory to Simulations. *Atoms*, 2017, 5 (3), 10.3390/atoms5030032 . hal-01643679

HAL Id: hal-01643679


<https://hal.science/hal-01643679>

Submitted on 21 Jun 2023

HAL is a multi-disciplinary open access archive for the deposit and dissemination of scientific research documents, whether they are published or not. The documents may come from teaching and research institutions in France or abroad, or from public or private research centers.

L'archive ouverte pluridisciplinaire **HAL**, est destinée au dépôt et à la diffusion de documents scientifiques de niveau recherche, publiés ou non, émanant des établissements d'enseignement et de recherche français ou étrangers, des laboratoires publics ou privés.

Stark Broadening from Impact Theory to Simulations

Roland Stamm ^{1,*}, Ibtissem Hannachi ^{1,2}, Mutia Meireni ¹, Laurence Godbert-Mouret ¹, Mohammed Koubiti ¹, Yannick Marandet ¹, Joël Rosato ¹, Milan S. Dimitrijević ³  and Zoran Simić ³

¹ Département de Physique, Aix-Marseille Université, CNRS, PIIM UMR 7345, 13397 Marseille CEDEX 20, France; ibtissem.hannachi@univ-amu.fr (I.H.); mutia_meireni@ymail.com (M.M.); laurence.mouret@univ-amu.fr (L.G.-M.); mohammed.koubiti@univ-amu.fr (M.K.); yannick.marandet@univ-amu.fr (Y.M.); joel.rosato@univ-amu.fr (J.R.)

² PRIMALAB, Faculty of Sciences, University of Batna 1, Batna 05000, Algeria

³ Astronomical Observatory, Volgina 7, 11060 Belgrade, Serbia; mdimitrijevic@aob.rs (M.S.D.); zsimic@aob.rs (Z.S.)

* Correspondence: roland.stamm@univ-amu.fr; Tel.: +33-491-288-621

Academic Editor: Ulrich Jentschura

Received: 31 August 2017; Accepted: 11 September 2017; Published: 20 September 2017

Abstract: Impact approximation is widely used for calculating Stark broadening in a plasma. We review its main features and different types of models that make use of it. We discuss recent developments, in particular a quantum approach used for both the emitter and the perturbers. Numerical simulations are a useful tool for gaining insight into the mechanisms at play in impact-broadening conditions. Our simple model allows the integration of the Schrödinger equation for an emitter submitted to a fluctuating electric field. We show how we can approach the impact results, and how we can investigate conditions beyond the impact approximation. The simple concepts developed in impact and simulation approaches enable the analysis of complex problems such as the effect of plasma rogue waves on hydrogen spectra.

Keywords: stark broadening; impact approximation; numerical simulation

1. Introduction

Stark profiles are used in astrophysics and other kinds of plasmas for obtaining information on the charged environment of the emitting particles. Using light for conveying information on the plasma often requires a modeling of both the plasma and the radiator. We will review different situations requiring different modeling approaches. The impact-broadening approach considers the emitter-plasma interaction as a sequence of brief separate collisions decorrelating the radiative dipole. Impact models are very effective for many types of plasmas, and can be applied to different kinds of emitters, hydrogen being an exception for most plasma conditions. Many different models using impact approximation have been developed, and we will review the most commonly-used. One can distinguish firstly between models keeping the quantum character of the perturbers, and those using a classical trajectory for the charged particles. Full quantum approaches require specific calculation techniques, which, once established, have proved to be of general interest. Another way to look at the models is the degree of accuracy required. It is often not necessary to have an accuracy better than about 20%, since the experimental errors are often of the same order or worse. This has enabled the development of a semi-empirical impact model, useful especially in cases where one does not have a sufficient set of atomic data for adequate application of more sophisticated methods with which one can readily obtain a large number of line shapes [1], making it an effective diagnostic tool.

A typical starting point for a line shape formalism in a plasma is a full quantum formalism for the emitter and the perturbers. It can be written as a linear response for the emitter dipole operator, and

provides the response of an emitter at a time t , knowing its state at an initial time [2]. This response in time allows the physical measurement of the spectrum to which it is linked by a Fourier transform. Quantum formalism introduces specific computational difficulties, but also brings powerful tools such as the angular averages. We will briefly discuss such approaches, and how they compare to semi-classical calculations. Classical path impact approximations have been widely developed, and exist in several levels of accuracy, depending on whether one is interested in a rapid analysis of a large number of spectra, or one asks for an accurate analysis of a few lines. We will identify situations for which other models are helpful, e.g., for the case where the emitter-perturber interactions cannot be represented by a sequence of collisions. Such models use the statistical properties of the electric field created by the perturbing particles. In astrophysics, model microfield methods provide an efficient alternative for cases where neither the impact nor the static approximation are valid. For such situations, several models have been developed and interfaced with atomic data. Their accuracy can be tested by simulation techniques avoiding some approximations, but at the expenses of computer time. Such computer simulations can be used to analyze the various physical processes involved in plasmas under arbitrary conditions. We will illustrate their use in the case of plasma rogue waves.

2. Impact Broadening

A detailed and accurate modeling of Stark broadening started almost sixty years ago with the development of a general impact theory having the ability of retaining the quantum character of the emitters and perturbers, and allowing both elastic and inelastic collisions between such particles [2]. The line shape is obtained by a Fourier transform of the dipole autocorrelation function (DAF), a quantity expressed as a trace over all possible states of the quantum emitter plus perturbers system:

$$C(t) = \text{Tr}[\vec{d} \cdot T^+(t) \vec{d} T(t) \rho], \quad (1)$$

where \vec{d} is the dipole moment of the emitter, $T(t) = \exp(-iHt/\hbar)$ the evolution operator and ρ the density matrix, these last two quantities being dependent on the Hamiltonian H for the whole system. Such an expression could be calculated by density functional theory or quantum Monte Carlo methods, taking advantage of the development of computational techniques and computer hardware [3]. Such studies have proved to be efficient for describing the properties of dense plasmas found in the interior of gaseous planets, the atmospheres of white dwarfs or the laboratory plasmas created by energetic lasers. They might be useful for understanding some features in the spectrum of such plasmas, but have not been developed yet in the context of line broadening. Probably the main reason for this is that there is no clear evidence that the dynamical effects of multiple quantum perturbers can affect a line shape. Another reason is that for most of the plasma conditions and line shapes studied, we can use the impact approximation, which assumes that the various perturbers interact separately with the emitter (binary collision assumption), and that the average collision is weak. A validity condition for the impact approximation is that the collision time is small compared with the decorrelation time of $C(t)$. If this condition and the binary collision assumptions are verified, it is possible to use a constant collision operator to account for all the effects of the perturbers on the emitter. Different approaches using impact approximation have been proposed, but we can distinguish firstly between quantum impact models that retain the quantum behavior of both emitters and perturbers, and the semiclassical impact models treating only the emitter as a quantum particle. A pictorial representation of the full quantum emitter-perturber interaction is provided by the use of wave packets for the perturbers. Each wave packet is scattered in a region within the reach of the interaction potential with the emitter. Quantum collision formalism can be applied, enabling the calculation of cross sections with the aid of scattering amplitudes. Although quantum impact calculations have been performed since the seventies [4,5], such calculations are not very numerous for line broadening due to their computational difficulty. In particular, they involve a calculation of the scattering matrix or S matrix [2].

Many calculations have been applied to isolated lines of various ions, a case for which the width w takes the compact form of an average over the perturbers after the use of the optical theorem [2]:

$$w = \frac{1}{2} N \{ v [\sigma_i + \sigma_f + \int d\Omega |f_i(\theta, \varphi) - f_f(\theta, \varphi)|^2] \}_{Av}, \quad (2)$$

where N is the perturbers' density, v their velocity, σ_i and σ_f are inelastic cross sections, f_i and f_f the forward-scattering amplitudes in a direction given by θ, φ for the initial i and final f states, and $\{\dots\}_{Av}$ stands for a Boltzmann thermal average.

With the advent of accurate atomic structure and S matrix codes, such impact quantum calculations have been given a new life [6,7], and are most often in good agreement with other calculations. A very efficient calculation has been proposed starting from Equation (2), using a Bethe-Born approximation [8] for evaluating inelastic cross sections. This semi-empirical model uses an effective Gaunt factor, a quantity which measures the probability of an incident electron changing its kinetic energy [9]. This function has been modified and improved to develop the modified semi-empirical model which is frequently used for calculations of isolated ion lines [1].

For most plasma conditions and line shapes studied, the wave packets associated with the perturbers are small and do not spread much in time. This enables the use of classical perturbers following classical paths. Different approaches use this approximation together with the impact approximation for the electron perturbers. Early calculations of hydrogen lines with comparisons to experimental profiles proved that a profile using an impact electron broadening [10], together with a static approximation for the ion perturbers, is in overall agreement for the Balmer H_β line in an arc plasma with a density $N = 2.2 \times 10^{22} \text{ m}^{-3}$ and a temperature $T = 10,400 \text{ K}$. The remaining discrepancies concerned the central part of the line and the far line wings, two regions that required an improvement of the model.

For isolated lines of neutral atoms and ions, the semiclassical perturbation (SCP) method [11] has been successfully applied to numerous lines, and is implemented in the STARK-B database [12]. The SCP method was inspired by developments in the quantum theory of collisions between atoms and electrons or ions, and, e.g., performs the angular averages with Clebsch-Gordan coefficients. It has the ability to generate several hundred lines rapidly for a set of densities and temperatures in a single run. The accuracy of the SCP method is assessed by a comparison to experimental spectra, and is about 20 to 30% for the widths of simple spectra, but could be worse for some complex spectra. The method is continuously improving, and has been interfaced with atomic structure codes [11].

An interesting point is raised by the comparison of impact quantum and semiclassical calculations, and a comparison of those with experiments. Quantum calculations have often been found to predict narrower lines than those of semiclassical models [13]. Semiclassical calculations may be brought closer to quantum widths, e.g., by a refined calculation of the minimum impact parameter allowing the use of a classical path [14]. Surprisingly, quantum widths of Li-like and boron-like ions often show a worse agreement with experiments than semiclassical calculation, thus calling for further calculations and analysis [7,15]. As an example of such, more recent quantum calculations [15] are in fairly good agreement with experiments [15].

3. Simulations of Impact Theory and Ion Dynamics

The need for a model that does not assume the impact approximation arose out of the study of hydrogen lines, with the surge of accurate profile measurements in near equilibrium plasmas [16]. It appeared that a standard model using a static ion approximation, and an impact electron collision operator, showed pronounced differences with the measures near the line centers, and also in the far wings. The line wings were well reproduced by the so-called unified theory, which retains the static interaction between an electron and the atom as a strong collision occurs [17,18]. The difference in the central part of the line was linked to the use of the static ion approximation, since it depended on the reduced mass of the emitter-ion perturber system. The observation of the Lyman- α (L_α) line [19]

showed later that the experimental profile was a factor 2.5 broader than the theoretical line using static ions in arc plasma conditions. This was a strong motivation for developing a technique able to retain ion dynamics in a context where the electric field is created by numerous ions in motion. Since perturbative approaches were unable to account for multiple strong collisions, a computer simulation has been proposed for describing the motion of the ions. The effect on the emitter of the time dependent ion electric field is obtained by a numerical integration of the Schrödinger equation. Early calculations showed the effect of ion dynamics in the central part of the line, and were able to strongly reduce the difference between experimental and simulation profiles [20–22].

Simple hydrogen plasma simulations may be used to illustrate the behavior of an electric field component during a time interval of the order of the line shape time of interest. This time is usually taken as the DAF decorrelation time, and can also be defined as the inverse of the line width. The electric field experienced by an atom surrounded by moving charged particles can be calculated at the center of a cubic box, using particles with straight line trajectories. The edge of the cube should be assumed to be equal to a few times the Debye length $\lambda_D = \sqrt{\epsilon_0 k_B T / (N e^2)}$, with T and N the hydrogen plasma temperature and density, respectively, e the electron charge, k_B the Boltzmann constant, and ϵ_0 the permittivity of free space. If we simulate only the ion perturbers, we assume that each particle creates a Debye shielded electric field, in an attempt to retain ion-electron correlations. Random number generators are used to obtain the uniform positions and Maxwell-Boltzmann distributed velocities of the charged particles. If an ion leaves the cubic box, it is replaced by a new one created near the cube boundaries. For the weak coupling conditions assumed, a large number of particles (several thousand commonly) is retained in a cube with a size larger than the Debye length. Such a model provides a good approximation for the time-dependent electric field in a weakly coupled ion plasma at equilibrium, although it suffers from inaccuracies, especially if the size of the box is not large enough [23]. We show in Figure 1 the time dependence of one component of the ionic electric field calculated at the center of the box for an electron density $N_e = 10^{19} \text{ m}^{-3}$, and a temperature $T = 40,000 \text{ K}$. The electric field is expressed in units of $E_0 = 1 / (4\pi\epsilon_0 r_0^2)$, where r_0 is the average distance between particles defined by $r_0^3 = 3 / (4\pi N_e)$. The time interval of 5 ns used in Figure 1a is the L_α time of interest for such plasma conditions. The validity condition of the binary collision approximation requests that the Weisskopf radius $\rho_w = \hbar n^2 / m_e v_i$, with n the principal quantum number of the L_α upper states ($n = 2$), and $v_i = \sqrt{2k_B T / m_p}$ the thermal ion velocity (m_e and m_p are resp. the electron and proton mass), is much smaller than the average distance between particles. This ratio is for L_α and protons of the order of 0.04, enabling the use of an impact approximation. The electric field in Figure 1a clearly exhibits several large fields that are well separated in time during the 5 ns of the L_α time of interest. During this time interval, only a few fields (3 in Figure 1a) have a magnitude larger than $50 E_0$, but about 20 have a magnitude of $10 E_0$ or more. A piece of the same field history is shown in Figure 1b during a time interval equal to the time of interest for the Balmer- β (H_β) line. For this time interval of 0.3 ns, the electric field shows much fewer fluctuations, the atom is no longer submitted to a sequence of sharp collisions, and we can no longer use the impact approximation. This is confirmed by a value of 0.16 for the ρ_w / r_0 ratio, making the use of an impact approximation for this line problematic. Looking now at Figure 1a,b, we can see a background of electric field fluctuations with a small magnitude of about E_0 , and a typical time scale longer than the collision time r_0 / v_i . Such fluctuations correspond to the sum of electric fields of distant particles with a magnitude on the order of E_0 . For hydrogen lines affected by the linear Stark effect, it is well known that this effect of weak collisions is dominant in near impact regimes [10], and results from the long range of the Coulomb electric field.

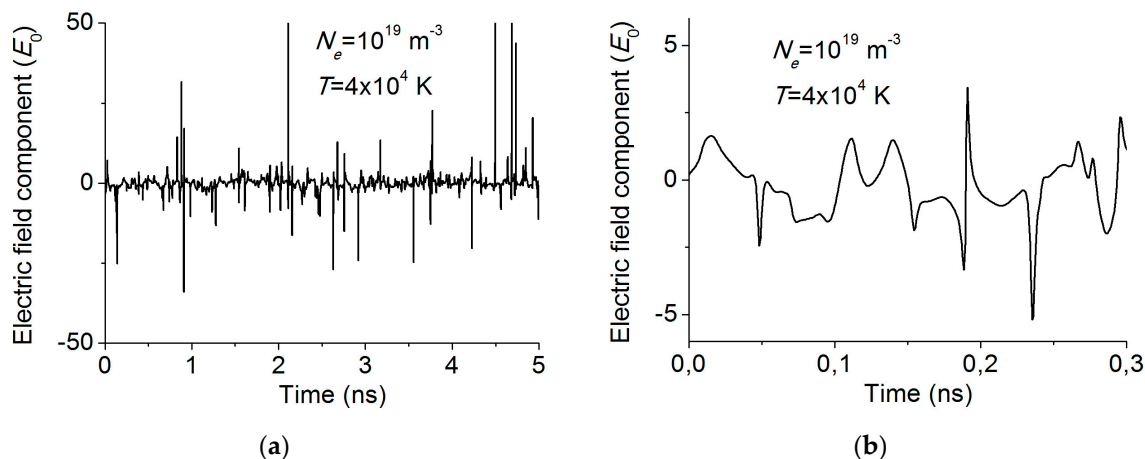


Figure 1. Electric field component in units of E_0 in a plasma with a density $N_e = 10^{19} \text{ m}^{-3}$, and a temperature $T = 40,000 \text{ K}$, during (a) a time interval of the order of the time of interest for the L_α line, and (b) a time interval of the order of the time of interest for the H_β line.

Using several thousand samples of such electric fields, it is possible to calculate the DAF for each line studied. This requires for each field history $\vec{E}(t)$ an integration of the Schrödinger equation of the emitter submitted to a dipolar interaction potential $-\vec{d} \cdot \vec{E}(t)$. We obtain the emitter’s evolution operator by finite difference computational methods, using time steps adjusted to ensure the best compromise between computer time cost and accuracy [24]. The integration time interval is provided by the time of interest for the line calculated, and a first estimate for the time step is a hundredth of the collision time. In the following, we retain only the broadening of the upper states of the line, resulting in some loss of accuracy for the first Balmer lines, but in a much faster calculation. We show in Figure 2a the DAF of L_α for the same plasma conditions as in Figure 1. The ab-initio DAF (solid line) is obtained by a simulation of the ions retaining also the effect of electrons with an impact approximation. We observe that this simulation is close to an impact calculation for both ions and electrons (dashed line). For the same condition and the H_β line, the decay of the ab-initio DAF is significantly smaller than for the impact calculation, indicating again a deviation from ion impact broadening for this line.

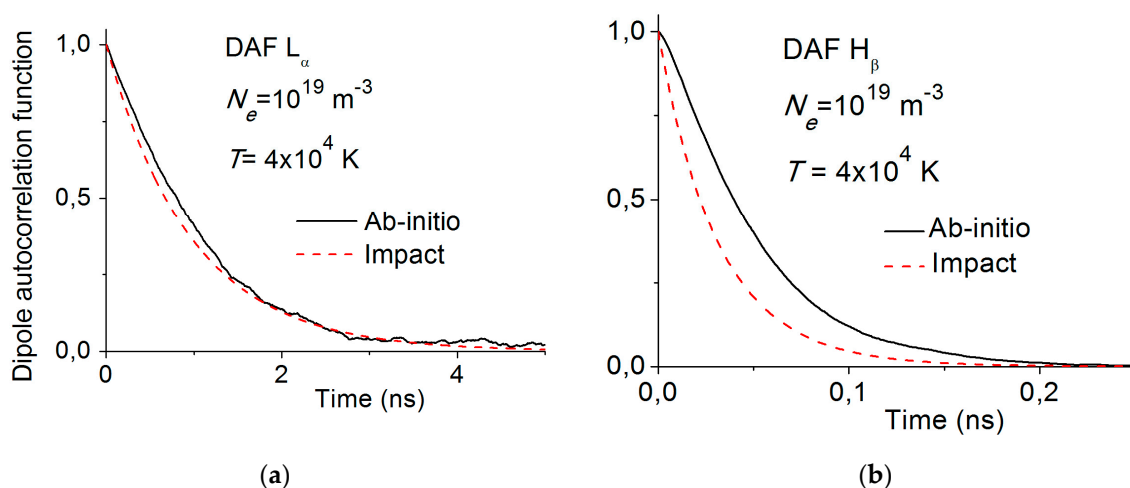


Figure 2. Dipole autocorrelation functions with an ab-initio simulation (solid line) and in the impact limit (dotted line) in a plasma with a density $N_e = 10^{19} \text{ m}^{-3}$, and a temperature $T = 40,000 \text{ K}$, for (a) the L_α Lyman transition, and (b) the H_β Balmer transition.

Another way of taking account of ion dynamics is with the help of stochastic processes. A stepwise constant stochastic process is used to model the electric field felt by the atom [25]. The process requires the knowledge of the microfield probability distribution function, and of a waiting time distribution function controlling the jumps from one field to the next one. Such model microfield methods are efficient for retaining ion dynamics effects, and are used for a diagnostic of hydrogen lines [26]. Stochastic processes are also used in the line shape code using the frequency fluctuation model for an inclusion of ion dynamics [27]. During the last decades, several simulations and models have been developed with the ability of retaining ion dynamics. The field is still active, with ion dynamics being one of the issues discussed in the Spectral Line Shapes in Plasmas workshop, providing many new analyses [28].

4. Effect of Plasma Waves

Plasmas sustain various types of waves, which behave differently in a linear and nonlinear regime. A way to distinguish between the two regimes is to calculate the ratio W of the wave energy density to the plasma energy density, given by:

$$W = \varepsilon_0 E_L^2 / 4N_e k_B T, \quad (3)$$

where E_L is the electric field magnitude of the wave. For values of W much smaller than 1, we expect a linear behavior of the waves. In a linear regime, electronic Langmuir waves oscillate at a frequency close to the plasma frequency $\omega_p = \sqrt{N_e e^2 / m_e \varepsilon_0}$, and can be excited even by thermal fluctuations. We assume that the numerous emitters on the line of sight are submitted to different Langmuir waves, each with the same frequency ω_p , but a different direction and phase chosen at random, and a magnitude sampled using a half-normal probability density function (PDF). In the following, we have used this half-normal PDF for the reduced electric field magnitude $F = E/E_0$:

$$P(F) = \frac{\sqrt{2}}{\sigma\sqrt{\pi}} \exp\left(-\frac{F^2}{2\sigma^2}\right) \quad (4)$$

In this expression, we use the standard deviation σ of a normal distribution, and thus obtain the mean value E_L of E by writing $E_L = \sigma E_0 \sqrt{2/\pi}$. Each Langmuir wave has a different electric field history, and we obtain the DAF by an average over about a thousand such field histories. For a plasma with a density $N_e = 10^{19} \text{ m}^{-3}$, and a temperature $T = 10^5 \text{ K}$, we first calculated the L_α DAF for Langmuir waves with a mean electric field magnitude corresponding to $W = 0.01$ ($E_L = 15E_0$). The response of the DAF is a periodic oscillation with a period equal to $2\pi/\omega_p$, but with an amplitude much smaller than 1 for this average field magnitude of $15E_0$. After a product with an impact DAF for retaining the effect of the background electron and ion plasma, there remains no visible effect of the waves on the convolution DAF for the value $W = 0.01$. This ratio can take much larger values, however; especially if an external energy source such as a beam of charged particles is present. As W increases, nonlinear phenomena start showing up, enabling, for instance, wave-wave couplings. Although only recently investigated in plasmas, the occurrence of rogue waves has been raised in various plasma conditions [29–31]. Rogue waves have been studied in many dynamical systems, and are known to the general public by the observation and study of rogue or freak waves that suddenly appear in the ocean as large isolated waves. In oceanography, rogue waves are defined as waves whose height is more than twice the mean of the largest third of the waves in a wave record. Rogue waves appear to be a unifying concept for studying localized excitations that exceed the strength of their background structures. They are studied in nonlinear optics [32], Bose-Einstein condensates [33], and many other fields outside of physics. For our line shape problem in plasmas, we postulate that nonlinear processes create rogue waves from a random background of smaller Langmuir waves. The physical mechanism at play is the coupling of the Langmuir wave with ion sound and electromagnetic waves; density fluctuations of the sound waves affect the high frequency waves through ω_p . The first Zakharov equation [34] shows how

density fluctuations affect Langmuir waves, and a second equation how a Langmuir wave packet can produce a density depression via the ponderomotive force [35]. We will not discuss these equations here, which are particularly useful for a study of wave collapse. Most present rogue wave studies rely on the nonlinear Schrödinger equation (NLSE), which is obtained in the adiabatic limit (slowly changing density perturbations) of the Zakharov equations [35]. A one-dimensional solution of the NLSE is commonly used to approximate the response of nonlinear media. Stable envelope solitons are possible solutions of the 1D NLSE. We will assume that there is a contribution of a stable envelope soliton for each history of the microfield, similarly to what we did for the background Langmuir wave. Using a ratio $W = 0.1$, the average peak magnitude of such solitons will be 3 times the amplitude of background Langmuir waves, fitting them in the category of rogue waves. A possible shape for the envelope is a Lorentzian, with a time dependence that bears some similarity with the celebrated Peregrine soliton [36]. We observe in Figure 3 that the DAF of L_α obtained with a product of the impact DAF and the Langmuir rogue wave DAF for $W = 0.1$ is affected by oscillations at the plasma frequency.

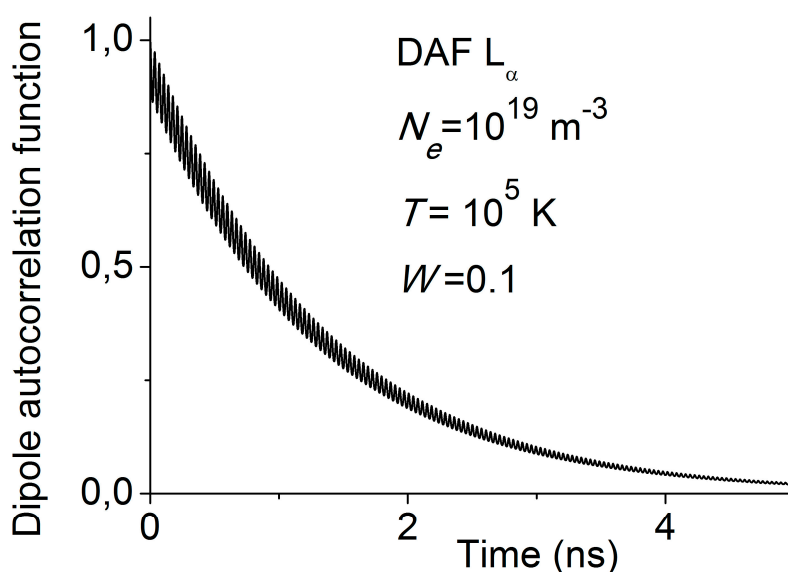


Figure 3. L_α dipole autocorrelation function in a plasma with a density $N_e = 10^{19} \text{ m}^{-3}$, and a temperature $T = 10^5 \text{ K}$, calculated with a product of the impact DAF and the Langmuir rogue wave DAF for $W = 0.1$.

Looking at the line shape obtained with a Fourier transform, we can see in Figure 4 that the peak of the line including the wave effect is about 10% lower than the impact line peak, but this with almost no effect on the line width. Not shown in Figure 4, we noticed that the wing of the line affected by rogue waves had a slightly slower decay than the impact profile, indicating a transfer of intensity from the center toward large line shifts. It is remarkable that a such rogue wave had a rather small effect on the profile. This is probably due to the fact that we are in impact conditions for this line. In impact regimes, decorrelation is very effective, leaving only a small broadening contribution to the type of rogue waves that we considered. A larger broadening effect would be observed by considering wave collapse, a phenomenon occurring as W takes larger values of the order of 1 or more for such plasma conditions. The emitters then experience the effect of a sequence of solitons which can significantly increase the broadening [37].

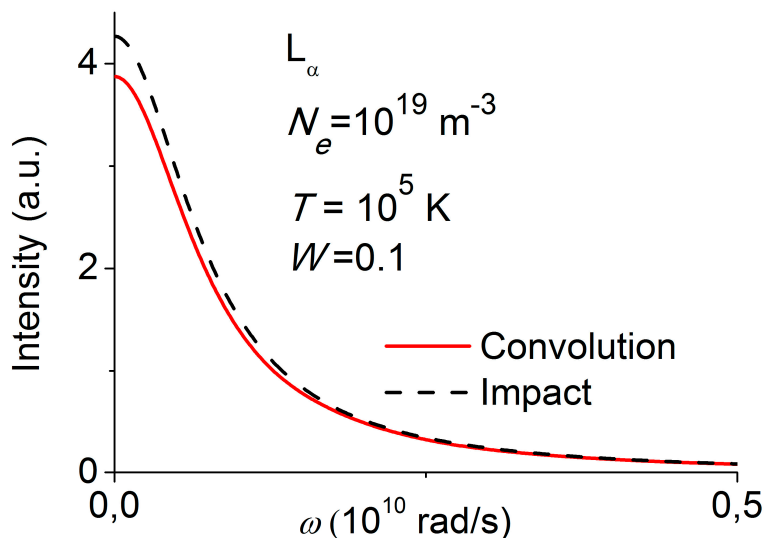


Figure 4. L_α in a plasma with a density $N_e = 10^{19} \text{ m}^{-3}$, and a temperature $T = 10^5 \text{ K}$, calculated with an impact approximation (dashed line), and with a Fourier transform of the DAF in Figure 3 (solid line).

5. Conclusions

Impact approximation mainly consists of saying that, on an average, it takes many collisions to change the quantum state of an atom. When this approximation is valid, the effect of the numerous fluctuating interactions of the emitter with the perturbers can be expressed with a constant collision operator. We have briefly described several models using impact approximation. A wide variety of impact models have been proposed, ranging from full quantum calculations to semiclassical approaches. Impact calculations allow expression of the width and shift of a line in terms of quantum scattering cross-sections. Such calculations have enabled many improvements in the application of quantum theory for obtaining observable quantities such as a line shape. The comparison between experimental and theoretical spectra is of great benefit for the validation of such models. It is thus crucial to be able to rapidly obtain numerous spectra for the lines of many atoms and ions. This is possible using models such as the semiclassical perturbation or the semi-empirical formalism. We have also shown how a computer simulation can reproduce the results of the impact approximation for hydrogen lines. Such simulations involve several thousand particles, however, and are certainly not the most efficient technique for obtaining the impact profile. The main advantage of simulations is that they can go beyond the impact approximation, for situations with many perturbers acting simultaneously on the emitter. We have briefly recalled the problem of ion dynamics, and have proposed a simple simulation for a calculation of the effect of Langmuir rogue waves of L_α in an impact regime.

Acknowledgments: This work is supported by the funding agency Campus France (Pavle Savic PHC project 36237PE). This work has also been carried out within the framework of the EUROfusion Consortium and has received funding from the Euratom research and training program 2014–2018 under Grant agreement no 633053. The views and opinions expressed herein do not necessarily reflect those of the European Commission.

Author Contributions: This work is based on the numerous contributions of all the authors.

Conflicts of Interest: The authors declare no conflict of interest.

References

1. Dimitrijević, M.S.; Konjević, N. Stark widths of doubly- and triply-ionized atom lines. *J. Quant. Spectrosc. Radiat. Transf.* **1980**, *24*, 451–459. [[CrossRef](#)]
2. Baranger, M. General Impact Theory of Pressure Broadening. *Phys. Rev.* **1958**, *112*, 855–865. [[CrossRef](#)]

3. McMahon, J.M.; Morales, M.A.; Pierleoni, C.; Ceperley, D.M. The properties of hydrogen and helium under extreme conditions. *Rev. Mod. Phys.* **2012**, *84*, 1607–1653. [[CrossRef](#)]
4. Barnes, K.S.; Peach, G. The shape and shift of the resonance line of Ca⁺ perturbed by electron collisions. *J. Phys. B* **1970**, *3*, 350–362. [[CrossRef](#)]
5. Bely, O.; Griem, H.R. Quantum-mechanical calculation for the electron-impact broadening of the resonance line of singly ionized magnesium. *Phys. Rev. A* **1970**, *1*, 97–105. [[CrossRef](#)]
6. Elabidi, H.; Ben Nessib, N.; Sahal-Bréchet, S. Quantum-mechanical calculations of the electron-impact broadening of spectral lines for intermediate coupling. *J. Phys. B* **2004**, *37*, 63–71. [[CrossRef](#)]
7. Elabidi, H.; Sahal-Bréchet, S.; Dimitrijević, M.S. Quantum Stark broadening of Ar XV lines. Strong collision and quadrupolar potential contributions. *Adv. Space Res.* **2014**, *54*, 1184–1189. [[CrossRef](#)]
8. Griem, H.R. Semi-empirical formulas for the electron-impact widths and shifts of isolated ion lines in plasmas. *Phys. Rev.* **1968**, *165*, 258–266. [[CrossRef](#)]
9. Van Regemorter, H. Rate of collisional excitation in stellar atmospheres. *Astrophys. J.* **1962**, *136*, 906–915. [[CrossRef](#)]
10. Griem, H.R.; Kolb, A.C.; Shen, K.Y. Stark broadening of hydrogen lines in a plasma. *Phys. Rev.* **1959**, *116*, 4–16. [[CrossRef](#)]
11. Sahal-Bréchet, S.; Dimitrijević, M.S.; Ben Nessib, N. Widths and shifts of isolated lines of neutral and ionized atoms perturbed by collisions with electrons and ions: An outline of the semiclassical perturbation (SCP) method and of the approximations used for the calculations. *Atoms* **2014**, *2*, 225–252. [[CrossRef](#)]
12. Sahal-Bréchet, S.; Dimitrijević, M.S.; Moreau, N. *STARK-B Database*; LERMA, Observatory of Paris, France and Astronomical Observatory: Belgrade, Serbia, 2014; Available online: <http://stark-b.obspm.fr> (accessed on 12 August 2017).
13. Griem, H.R. *Principles of Plasma Spectroscopy*; Cambridge University Press: Cambridge, UK, 1997.
14. Alexiou, S.; Lee, R.W. Semiclassical calculations of line broadening in plasmas: Comparison with quantal results. *J. Quant. Spectrosc. Radiat. Transf.* **2006**, *99*, 10–20. [[CrossRef](#)]
15. Elabidi, H.; Sahal-Bréchet, S.; Ben Nessib, N. Quantum Stark broadening of the 3s-3p spectral lines in Li-like ions; Z-scaling and comparison with semi-classical perturbation theory. *Eur. Phys. J. D* **2009**, *54*, 51–64. [[CrossRef](#)]
16. Wiese, W.L.; Kelleher, D.E.; Paquette, D.R. Detailed study of the Stark broadening of Balmer lines in a high density plasma. *Phys. Rev. A* **1972**, *6*, 1132–1153. [[CrossRef](#)]
17. Voslamber, D. Unified model for Stark broadening. *Z. Naturforsch.* **1969**, *24*, 1458–1472.
18. Smith, E.W.; Cooper, J.; Vidal, C.R. Unified classical-path treatment of Stark broadening in plasmas. *Phys. Rev.* **1969**, *185*, 140–151. [[CrossRef](#)]
19. Grützmacher, K.; Wende, B. Discrepancies between the Stark-broadening theories of hydrogen and measurements of Lyman- α Stark profiles in a dense equilibrium plasma. *Phys. Rev. A* **1977**, *16*, 243–246. [[CrossRef](#)]
20. Stamm, R.; Voslamber, D. On the role of ion dynamics in the Stark broadening of hydrogen lines. *J. Quant. Spectrosc. Radiat. Transf.* **1979**, *22*, 599–609. [[CrossRef](#)]
21. Stamm, R.; Smith, E.W.; Talin, B. Study of hydrogen Stark profiles by means of computer simulation. *Phys. Rev. A* **1984**, *30*, 2039–2046. [[CrossRef](#)]
22. Stamm, R.; Talin, B.; Pollock, E.L.; Iglesias, C.A. Ion-dynamics effects on the line shapes of hydrogenic emitters in plasmas. *Phys. Rev. A* **1986**, *34*, 4144–4152. [[CrossRef](#)]
23. Rosato, J.; Capes, H.; Stamm, R. Ideal Coulomb plasma approximation in line shapes models: Problematic issues. *Atoms* **2014**, *2*, 253–258. [[CrossRef](#)]
24. Vesely, F. *Computational Physics, an Introduction*; Plenum Press: New York, NY, USA, 1994.
25. Brissaud, A.; Frisch, U. Theory of Stark broadening-II exact line profile with model microfield. *J. Quant. Spectrosc. Radiat. Transf.* **1971**, *11*, 1767–1783. [[CrossRef](#)]
26. Stehlé, C. Stark broadening of hydrogen Lyman and Balmer in the conditions of stellar envelopes. *Astron. Astrophys. Suppl. Ser.* **1994**, *104*, 509–527.
27. Talin, B.; Calisti, A.; Godbert, L.; Stamm, R.; Lee, R.W.; Klein, L. Frequency-fluctuation model for line-shape calculations in plasma spectroscopy. *Phys. Rev. A* **1995**, *51*, 1918–1928. [[CrossRef](#)] [[PubMed](#)]
28. Spectral Line Shapes in Plasmas (SLSP) Code Comparison Workshop. Available online: <http://plasma-gate.weizmann.ac.il/slsp/> (accessed on 20 July 2017).

29. Moslem, W.M.; Shukla, P.K.; Eliasson, B. Surface plasma rogue waves. *EPL* **2011**, *96*, 25002. [[CrossRef](#)]
30. Ahmed, S.M.; Metwally, M.S.; El-Hafeez, S.A.; Moslem, W.M. On the generation of rogue waves in dusty plasmas due to modulation instability of nonlinear Schrödinger equation. *Appl. Math Inf. Sci.* **2016**, *10*, 317–323. [[CrossRef](#)]
31. Mc Kerr, M.; Kourakis, I.; Haas, F. Freak waves and electrostatic wavepacket modulation in a quantum electron–positron–ion plasma. *Plasma Phys. Control. Fusion* **2014**, *56*, 035007. [[CrossRef](#)]
32. Erkintalo, M.; Genty, G.; Dudley, J.M. Rogue-wave-like characteristics in femtosecond supercontinuum generation. *Opt. Lett.* **2009**, *34*, 2468–2470. [[CrossRef](#)] [[PubMed](#)]
33. Bludov, Y.V.; Konotop, V.V.; Akhmediev, N. Matter rogue waves. *Phys. Rev. A* **2009**, *80*, 033610. [[CrossRef](#)]
34. Zakharov, V.E. Collapse of Langmuir waves. *Sov. Phys. JETP* **1972**, *35*, 908–914.
35. Robinson, P.A. Nonlinear wave collapse and strong turbulence. *Rev. Mod. Phys.* **1997**, *69*, 507–573. [[CrossRef](#)]
36. Bailung, H.; Sharma, S.K.; Nakamura, Y. Observation of Peregrine solitons in a multicomponent plasma with negative ions. *Phys. Rev. Lett.* **2011**, *107*, 255005. [[CrossRef](#)] [[PubMed](#)]
37. Hannachi, I.; Stamm, R.; Rosato, J.; Marandet, Y. Effect of nonlinear wave collapse on line shapes in a plasma. *EPL* **2016**, *114*, 23002. [[CrossRef](#)]



© 2017 by the authors. Licensee MDPI, Basel, Switzerland. This article is an open access article distributed under the terms and conditions of the Creative Commons Attribution (CC BY) license (<http://creativecommons.org/licenses/by/4.0/>).